Simulation study of membrane supported oxidation of methane with simultaneous steam reforming using O_2-selective Perowskite hollow fibres

C. Hamel[1], H. Wang[2], J. Caro[2], E. Tsotsas[3], A. Seidel-Morgenstern[1,3]

[1] Max-Planck-Institut für Dynamik komplexer technischer Systeme, D-39106 Magdeburg, Germany
[2] Universität Hannover, Institut für Physikalische Chemie und Elektrochemie, D-30167 Hannover
[3] Otto-von-Guericke-Universität, Institut für Verfahrenstechnik, D-39106 Magdeburg, Germany

Abstract

The partial oxidation of methane to synthesis gas was investigated in a novel type of perm selective membrane reactor using Perowskite hollow fibers. The operating behaviour of this membrane reactor integrating the process steps selective separation of oxygen from air, selective O_2 transfer in the membrane and oxidation of methane with simultaneous steam reforming was investigated theoretically by means of detailed 2D models and evaluated with performed experiments.

Keywords: Synthesis gas, Perowskite hollow fibres, membrane reactors, modelling

1. Introduction

The generation of synthesis gas from methane is currently performed by conventional steam reforming or by partial oxidation (POX) in fixed-bed reactors using nickel or noble metal based catalysts at temperatures around 900°C. In the last years several new reactor concepts were suggested to improve in particular the heat exchange, e.g. auto thermal reformers, catalytic coated wall reactors, fluidised bed or membrane reactors [1]. Improved POX of methane is currently a very promising direction for better generation of synthesis gas, in particular if oxygen is fed in a distributed manner separated from air using O_2-selective mixed conducting membranes. The industrial applicability of this concept depends on the availability of suitable selective tubular membranes characterised by thin walls to intensify the mass and heat transfer. In addition to the desired slightly exothermic partial oxidation in such reactors also the highly exothermic total oxidation can take place. The related heat generation can be exploited by coupling with conventional endothermal steam reforming to realise an auto thermal operating mode.

2. Results and Discussion

On the basis of experimental results using the novel BCFZ hollow fiber membrane ($BaCo_xFe_yZr_zO_{3-\delta}$, BCFZ, produced by spinning [2]) the operating behavior of a membrane reactor integrating the process steps air separation, selective O_2 transfer in the BCFZ, and oxidation of methane with simultaneous steam reforming was evaluated. The coupling of the mass balances of the synthesis gas side (shell side, ss) and the air providing side (tube side, ts) and the description of mass transfer in the O_2-selective perovskite hollow fibers was analyzed using reduced reactor models. The estimation and validation of mass transfer parameters for the characterization of the membrane was based on systematic experiments [3,4]. The Wagner approach was used to describe the oxygen permeation flux, J_i, through the BCFZ perovskite hollow fiber. The perovskite hollow fiber is 100% selective for oxygen, thus J_i is J_{O2}.

$$J_{O_2} = \frac{D_{eff}}{4 \cdot n \cdot t} \cdot \left[\left(P_{O_2}^{ss} \right)^n - \left(P_{O_2}^{ts} \right)^n \right] \qquad \text{with} \qquad D_{eff} = D_\infty \cdot e^{-\frac{E_A}{R \cdot T}}$$

Where D_{eff} is the effective diffusion coefficient of the perovskite material, t is the thickness of the hollow fiber, P_{O2} is the O_2 partial pressure on the tube and shell sides, D_∞ is the preexponential factor, and E_A is the activation energy. For the determination of the oxygen transport coefficients for the perovskite hollow fiber under study, it turned out necessary to vary the oxygen partial pressure on the feed and permeate sides at different temperatures. This can be easily done using pressurized air on the feed side of the membrane and synthetic air of 1 bar with a different oxygen content on the permeate side as a sweep. A comparison between the results of these mass transfer experiments and simulations is given in figure 1.

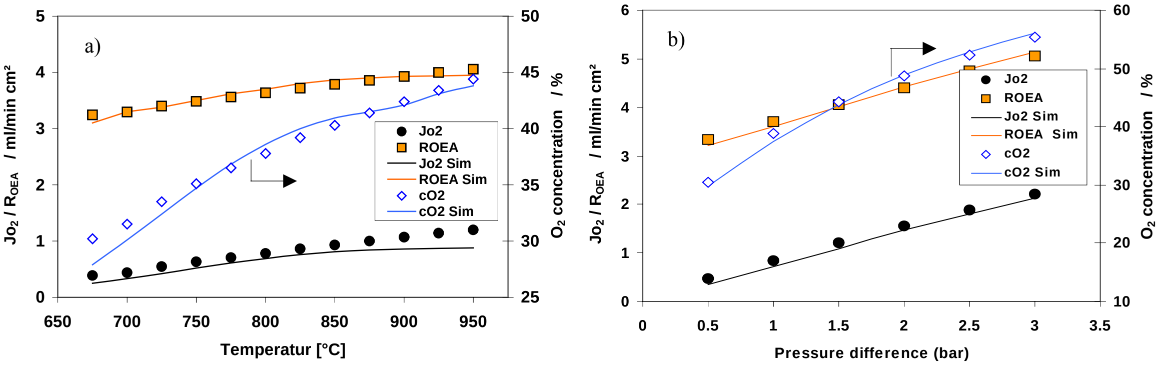

Figure 1: O_2 permeation rates, J_{O2}, O_2-enriched air production rates, R_{OEA}, and O_2 concentrations. Co_2 was realized using the total pressure gradients (experiments *symbols*; simulations *lines*). The conditions were as follows: membrane area. 3.50 cm^2; initial air fluxes feed side. 100 mL min^{-1}, permeate side. 10 mL min^{-1}. (a) Pressure difference of 1.5 bar. (b) Temperature of 950 °C.

A sufficient agreement concerning the influence of temperature (a) and oxygen partial pressure (b) on the oxygen flux in the membrane was obtained. These results also demonstrate the potential of the fibers used to produce oxygen enriched air as it is used, e.g., in industrial furnaces, the Claus process, and the fluid cracking catalysis (FCC) catalyst regeneration.

The derived equations describing the mass transport in the membrane as well as kinetic approaches for the rates of oxidation and steam reforming of methane coming from the literature [5-7] were implemented in a detailed two-dimensional pseudo-homogeneous reactor model using the simulation tool COMSOL®. The derived model allows the consideration and calculation for the usage of reactive sweep gases and the oxidation-reforming process, respectively. Under the assumptions of steady state and pseudo-homogeneous, ideal gas behavior, the mass and heat balances can be formulated:

Component mass balance:

$$0 = \frac{1}{r}\cdot\frac{\partial}{\partial r}\left[D_r(r)\cdot r\cdot\frac{\partial c_i}{\partial r}\right] + D_z\cdot\frac{\partial^2 c_i}{\partial z^2} - \cdot\frac{\partial\left(u_z\cdot c_i\right)}{\partial z} - \frac{1}{r}\cdot\frac{\partial\left(r\cdot u_r\cdot c_i\right)}{\partial r} + \frac{1-\psi(r)}{1-\bar{\psi}}\cdot\sum_j \nu_{ij}\cdot r_j$$

$$\text{BC:}\quad r = 0:\ \frac{\partial c_i}{\partial r} = 0;\quad r = R:\ J_i = -D_r\cdot\frac{\partial c_i}{\partial r}(r = R)$$

Where D_r/ D_z is the radial/ axial mass dispersion coefficient [8], c_i is the concentration of component i, u_r/ u_z is the radial/ axial direction of the velocity vector, ψ is the porosity of the catalyst bed, ν_{ij} is the stoichiometric coefficient of component i for reaction j, and r_j is the reaction rate for reaction j.

Heat balance:

$$0 = -\frac{1}{r}\frac{\partial}{\partial r}\left[\lambda_r(r)\cdot r\cdot\frac{\partial T}{\partial r}\right] + \lambda_z\frac{\partial^2 T}{\partial z^2} - c_p\cdot\frac{\partial\left(\rho u_z T\right)}{\partial z} - c_p\cdot\frac{1}{r}\left[\cdot\frac{\partial\left(r\rho u_r T\right)}{\partial r}\right] + \frac{1-\psi(r)}{1-\bar{\psi}}\cdot\sum_j\left(-\Delta H_{Rj}\right)\cdot r_j$$

$$\text{BC:}\quad r = 0:\ \frac{\partial T}{\partial r} = 0;\quad r = R:\ \dot{q} = -\lambda_r\cdot\frac{\partial T}{\partial r} + \rho\cdot c_p\cdot u_r\cdot T$$

Where λ_r/ λ_z is the radial/ axial heat dispersion coefficient [8], ρ is the density, c_p is the specific heat capacity, ΔH_{Rj} is the reaction enthalpy of reaction j, and T is the temperature.

To calculate the flow field under reactive conditions the extended Navier Stokes equation and the mass continuity equation were solved. The friction force arising due to the flow through the packed bed was calculated according to Ergun [9] by defining the friction coefficient. For the simplified reduced one-dimensional model negligible axial and radial dispersion and plug-flow conditions were assumed.

Mathematical modeling was carried out to be indispensable for the proper operation of the membrane reactor. Comparing with predictions of the reduced approach, the two-dimensional (2D) model was found necessary for a detailed analysis of the pronounced concentration, temperature, and velocity fields. In figure 2 are illustrated configurations of the membrane reactor with a catalyst bed (b) and a catalyst coated hollow fiber (a). In both cases, the fiber separates the reactor in the air (tube) and synthesis gas (shell) sides. Depending on the catalyst arrangement the hot spot obtained can be located directly on the membrane, which leads under unfavourable operation conditions to an inactivation or melting of the hollow fibre. Additionally, the complex temperature fields are depicted for the considered reactor configurations as predicted with the reduced 1D (c) and detailed 2D models (d, e). As can be seen from figure 2 the essential temperature effects and the performance of the investigated concept can be described only using the more detailed two dimensional reactor model.

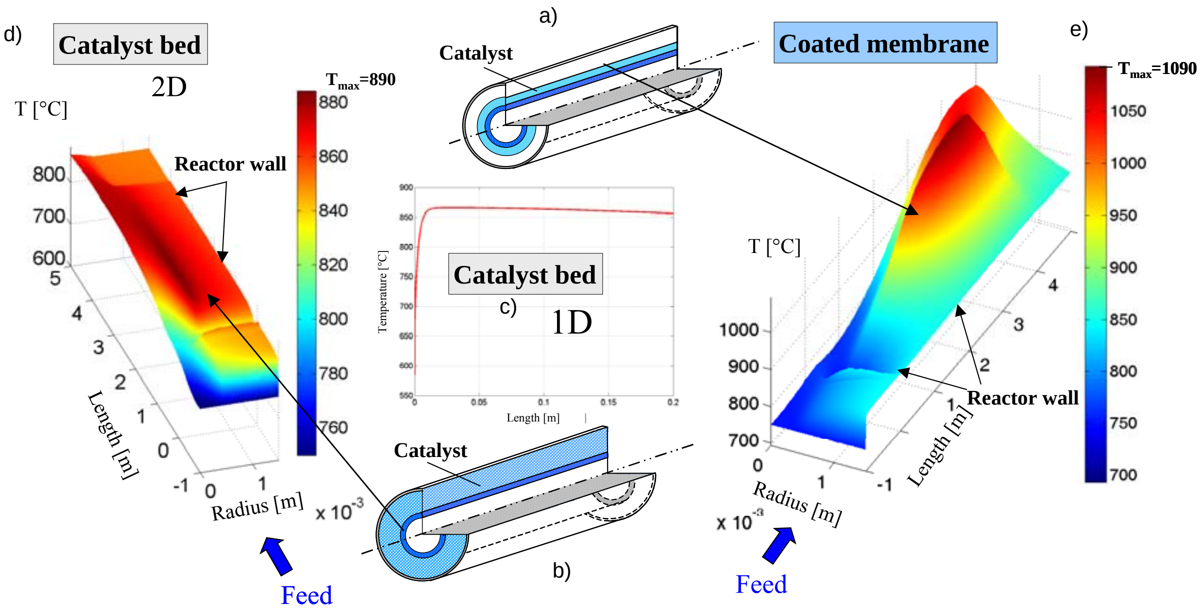

Figure 2: Membrane reactor set up investigated (a and b) and temperature profiles predicted using 1D (c) and 2D models (d,e) Simulation parameters: membrane surface area =3.50cm^2, T_{in}=750°C, T_{wall}=850°C, m_{cat}=500mg, catalyst particle size=0.28mm, tube side: pressure p=2bar, air flow rate V_{air}=150ml/min, shell side: p= 40bar, feed flow rate V_{air}=30 ml/min.

Based on extensive kinetic measurements a modification of the reaction network given in [5,6,10] and an estimation of suitable kinetic parameters for the used catalyst was possible. Furthermore, the derived data were implemented in the mathematical model described above.

In figure 3 selected results obtained in a laboratory-scale reactor are illustrated which could be operated for several hundred hours in the partial oxidation reaction. These experimental results allow further a validation of the estimated kinetic parameters and the developed detailed reactor model.

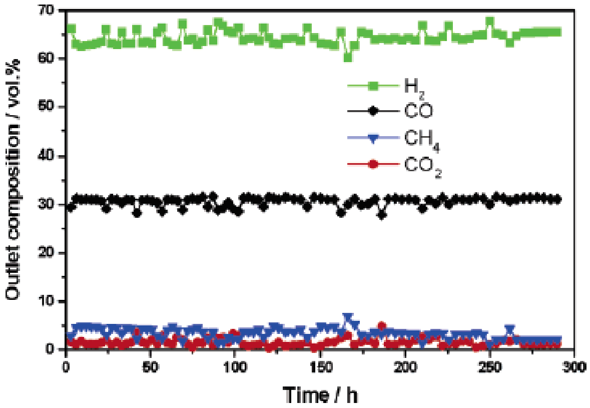

Figure 3: Off-gas composition in the POX. The gas composition (65% H_2, 31% CO, 2.5% CH_4, and 1.5% CO_2) corresponds to $X(CH_4)$=95%; $S(CO)$=96%; $S(CO_2)$=4%; Parameters: $T_{in}=T_{wall}$=875°C, tube side: pressure p=1bar, air flow rate V_{air}=150ml/min, shell side: p= 1bar, feed flow rate V_{CH4}=55 ml/min, V_{H2O}=5 ml/min

The corresponding simulation results as a function of the axial and radial coordinate are given in figure 4. Obviously the highest conversion of methane and concentration of CO_2 can be obtained closed to the membrane surface (see figure 4a,d) where the concentration of oxygen is maximum too. Thus, CO_2 is formed as a primary product. In a second step CO_2 is converted to CO and H_2 by dry reforming with methane. On the basis of the experimental and by simulations generated data the conclusions of [11-12] could be confirmed. Thus, the formal partial oxidation of methane consists in a mechanism of total oxidation of methane with a subsequent steam and dry reforming, respectively. The detailed 2D reactor model describes the reactor performance and the outlet molar fractions very well (see table 1). The obtained hot spot (figure 4e) leads to a higher temperature level and higher conversion compared to the experiments.

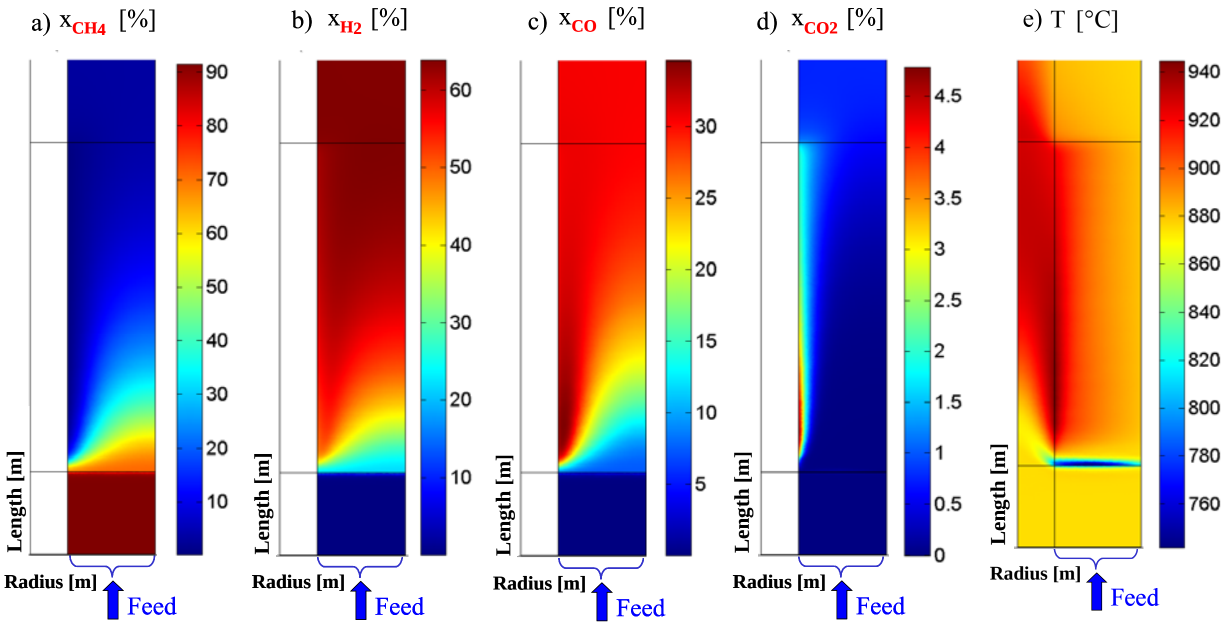

Figure 4. Concentration and temperature fields in the membrane reactor, Simulation parameters: $T_{in}=T_{wall}=875°C$, tube side: pressure p=1bar, air flow rate $V_{air}=150$ml/min, shell side: p= 1bar, feed flow rate $V_{CH4}=55$ ml/min, $V_{H2O}=5$ ml/min

Table 1: Comparison of experiment and simulation

	XCH_4	**SCO**	**SCO_2**	**H_2/CO**	**xCH_4^{out}**	**xH_2^{out}**	**xCO^{out}**	**xCO_2^{out}**	**xO_2^{out}**	**xH_2O^{aus}**
	[%]	[%]	[%]	[-]	[%]	[%]	[%]	[%]	[%]	[%]
Experiment	95	96	4	2,1	2.5	65	31	1,5	0	0
2D-simulation	97	97	3	2,1	2,3	63,9	31	0,8	0	2

3. Summary

Considering a new type of mixed conducting hollow fibre the operating behaviour of a membrane reactor integrating the process steps air separation, selective O_2 transfer in the membrane and oxidation of methane with simultaneous steam reforming was investigated theoretically. Different arrangements of the used catalyst in the membrane reactor were evaluated in a broad range of operation conditions by means of reduced 1D and detailed 2D reactor models

References

[1] Stitt, E.H., Trans IChemE A, Chem. Eng. Res. and Des., 82 (A2), 2004, 129-139

[2] Schiestel, T.; Kilgus, M.; Peter, S.; Caspary, K. J.; Wang, H. H.; Caro, J., J.Membr. Sci. 2005, 258, 1

[3] Wang, H., Caro, J.; Werth, S.; Schiestel, T., Angew. Chem., Int. Ed. 2005, 44, 2.

[4] Hamel, C., Seidel-Morgenstern, A., Schiestel, T., Werth, S., Tablet, C., Caro, J., Wang, H., AIChE J., 52, 2006, 3118-3125

[5] Hou, K., Hughes, R., CEJ, 82, 2001, 311-328

[6] Xu, J.,Froment, G, AIChE J., 35, 1989, 88-96

[7] Smet, C.R.H., de Croon, M.H.J.M., Berger, R.J., Marin, G.B., Schouten, J.C., Appl.Catal. A, 187, 1999, 33-48

[8] Tsotsas, E., VDI-Wärmeatlas, Verein Deutscher Ingenieure, 1997 chapter Mh

[9] Ergun, S., Chem. Eng. Progress., 1952, 35, 89-94

[10] Ashcroft, A.T., Cheetham, A.K., Green, M.L.H., Vernon, P.D.F., Nature, 352, 6332, (1991), 225

[11] Caro, J., Chemie Ingenieur Technik 2006, 78, 899

[12] Chen, C.S., Feng, S.J., Ran, S., Zhu, D.C., Lin, W., Bouwmeester, H.J.M., Angew. Chem. Int. Ed. 2003, 42, 5196